How Strong Is Hydrogen Bonding in Ionic Liquids? Combined X-ray Crystallographic, Infrared/Raman Spectroscopic, and Density Functional Theory Study

ARTICLE *in* THE JOURNAL OF PHYSICAL CHEMISTRY B · JULY 2013

Impact Factor: 3.3 · DOI: 10.1021/jp405255w · Source: PubMed

THE JOURNAL OF PHYSICAL CHEMISTRY B

Article

pubs.acs.org/JPCB

How Strong Is Hydrogen Bonding in Ionic Liquids? Combined X-ray Crystallographic, Infrared/Raman Spectroscopic, and Density Functional Theory Study

Sergey A. Katsyuba,*[,†] Mikhail V. Vener,[‡] Elena E. Zvereva,[†] Zhaofu Fei,[§] Rosario Scopelliti,[§] Gabor Laurenczy,[§] Ning Yan,[§] Emilia Paunescu,[§] and Paul J. Dyson*[,§]

[†]A. E. Arbuzov Institute of Organic and Physical Chemistry of Kazan Scientific Centre of the Russian Academy of Sciences, Arbuzov str. 8, 420088 Kazan, Russia

[‡]Department of Quantum Chemistry, Mendeleev University of Chemical Technology, Miusskaya Square 9, 125047 Moscow, Russia

[§]Laboratory of Organometallic and Medicinal Chemistry, Institut des Sciences et Ingénierie Chimiques, Ecole Polytechnique Fédérale de Lausanne (EPFL) EPFL−BCH, CH-1015 Lausanne, Switzerland

Supporting Information

ABSTRACT: Hydrogen bonding in ionic liquids based on the 1-(2′-hydroxylethyl)-3-methylimidazolium cation ($[C_2OHmim]^+$) and various anions ($[A]^-$) of differing H-bond acceptor strength, viz. hexafluorophosphate $[PF_6]^-$, tetrafluoroborate $[BF_4]^-$, bis(trifluoromethanesulfonimide) $[Tf_2N]^-$, trifluoromethylsulfonate $[OTf]^-$, and trifluoroacetate $[TFA]^-$, was studied by a range of spectroscopic and computational techniques and, in the case of $[C_2OHmim][PF_6]$, by single crystal X-ray diffraction. The first quantitative estimates of the energy (E_{HB}) and the enthalpy ($-\Delta H_{HB}$) of H-bonds in bulk ILs were obtained from a theoretical analysis of the solid-state electron-density map of crystalline $[C_2OHmim][PF_6]$ and an analysis of the IR spectra in crystal and liquid samples. E_{HB} for OH···$[PF_6]^-$ H-bonds amounts to ∼3.4−3.8 kcal·mol^{-1}, whereas weaker H-bonds (2.8−3.1 kcal·mol^{-1}) are formed between aromatic C2H group of imidazolium ring and the $[PF_6]^-$ anion. The enthalpy of the OH···$[A]^-$ H-bonds follows the order: $[PF_6]$ (2.4 kcal·mol^{-1}) < $[BF_4]$ (3.3 kcal·mol^{-1}) < $[Tf_2N]$ (3.4 kcal·mol^{-1}) < [OTf] (4.7 kcal·mol^{-1}l) < [TFA] (6.2 kcal·mol^{-1}). The formation of aggregates of self-associated $[C_2OHmim]^+$ cations is present in liquid $[C_2OHmim][PF_6]$, $[C_2OHmim][BF_4]$, and $[C_2OHmim][Tf_2N]$, with the energy of the OH···OH H-bonds amounting to ∼6 kcal·mol^{-1}. Multiple secondary interactions in the bulk ILs influence their structure, vibrational spectra, and H-bond strength. In particular, these interactions can blue-shift the stretching frequencies of the CH groups of the imidazolium ring in spite of red-shifting CH···$[A]^-$ H-bonds. They also weaken the H-bonding in the IL relative to the isolated ion pairs, with these anticooperative effects amounting to ca. 50% of the E_{HB} value.

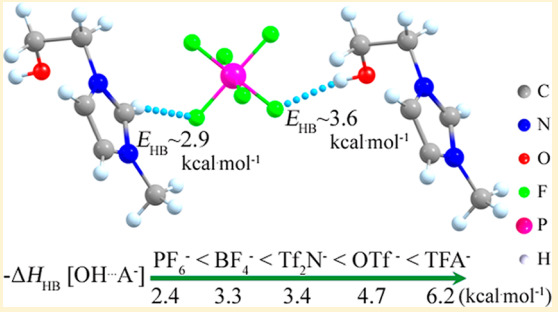

INTRODUCTION

Hydrogen bonds (H-bonds) have been suggested to be one of the molecular features which determine the properties of ionic liquids (ILs).[1−3] Consequently, a plethora of theoretical and experimental studies have been devoted to hydrogen bonding in ILs.[2,4−7] Despite these studies the relative importance of the H-bonding compared to other interactions is still a key area of debate. While some authors attribute a crucial role to H-bonding, others consider its relevance minor compared with the role of pure electrostatic interactions.[3,8−13] One of the main problems with discussions of this kind is the absence of energetic characteristics of H-bonds in ILs, where separation of H-bonding from the Coulombic interaction of the ions is extremely difficult. Quantum-chemical computations, usually applied for the most straightforward estimation of the strength of H-bonding between two molecules in vacuum, are inadequate in the case of the pairwise interaction of two counterions that are also able to form an H-bond between each other. The computed binding energy (BE) of such ion pairs includes not only effects of the H-bond formation but also "pure" Coulombic attraction of two opposite charges. As a result, BEs typically amount to ca. 100 kcal·mol^{-1}, which is well-beyond the limits of H-bond energies. Moreover, H-bond energies cannot be extracted from experimental measurement of the dissociation energies of ion pairs.

As a consequence of such a situation, the description of H-bonds in ILs at present is limited to their geometrical or spectroscopic characteristics.[2,3,6,9,14−24] The two main ways used to give (quantitative) estimates of the strength of H-bonds in condensed-phase systems comprise the following: (i) the use

Received: May 28, 2013
Revised: July 3, 2013
Published: July 3, 2013

   dx.doi.org/10.1021/jp405255w | J. Phys. Chem. B 2013, 117, 9094−9105

of spectroscopic indicators of H-bond formation such as red-shifts of X-H stretching vibrational frequencies (νXH) or increases in IR intensities[25,26] and (ii) the application of quantum theory of atoms in molecules and crystals.[27,28] It should be noted that a red shift and strengthening of the νXH IR band along with the (3,−1) critical point is one of the well-accepted criteria of the H-bond formation.[29] Both approaches allow the energy (E_{HB}) or enthalpy ($-\Delta H_{HB}$) of an H-bond to be estimated via the application of empirical relationships calibrated on independent and reliable data of different methods in cases when unequivocal determination of either E_{HB} or $-\Delta H_{HB}$ is possible. In particular, two relationships (1 and 2 below)[25] are used to evaluate the enthalpies of intermolecular H-bonds in liquids, solids and solutions:

$$-\Delta H_{HB}[\text{kcal}\cdot\text{mol}^{-1}] = 0.29\Delta I^{1/2}[\text{km mol}^{-1}] \quad (1)$$

Here, $\Delta I^{1/2} = I^{1/2} - I_0^{1/2}$, where I is the IR intensity for the localized, uncoupled stretching vibration (νXH) of the X-H group participating in the H-bond as compared to the noninteracting group (I_0). Equation 1 is applicable to 1:1 H-bonded complexes in which the $-\Delta H_{HB}/E_{HB}$ values are lower than 15 kcal·mol^{-1}. In molecular complexes with strong H-bonds ($-\Delta H_{HB}/E_{HB}$ > 15 kcal·mol^{-1}) the I value is inversely proportional to the O···X distance (X = O, N)[30,31] and applicability of this equation becomes problematic.

$$-\Delta H_{HB}[\text{kcal mol}^{-1}] = 0.33(\Delta\nu[\text{cm}^{-1}] - 40)^{1/2} \quad (2)$$

where $\Delta\nu = \nu XH^{free} - \nu XH^{bonded}$ represents the red-shift value of the νXH frequency caused by the formation of the H-bond with the XH group being the proton donor. In contrast to the I value, which depends solely on the strength of the H-bond, the $\Delta\nu$ value also depends on environmental effects, e.g., temperature.[32] Probably, this is why the $\Delta\nu - \Delta H_{HB}$ approach appears to be less accurate than that obtained with eq 1.[25]

Equations 1 and 2 were obtained for a series of neutral H-bonded systems. Applicability of eq 1 to ionic species is vague.[25] On the other hand, eq 2 was successfully applied for estimation of H-bonded enthalpies in ionic species and zwitterions, e.g., see refs 32 and 33.

In crystals with X−H···O H-bonds (X = O, N, and C), E_{HB} can be estimated[34] using the local electronic potential energy density, V_b, at the H···O bond critical point in electron density.[27]

$$E_{HB}[\text{kcal mol}^{-1}] = -314V_b[\text{atomic units}] \quad (3)$$

An expression, which links E_{HB} with the local electronic kinetic energy density G_b, has also been proposed:[35]

$$E_{HB}[\text{kcal mol}^{-1}] = 269G_b[\text{atomic units}] \quad (4)$$

The relevance of this expression for crystals with intermolecular hydrogen bonds of different types and strength has been recently demonstrated.[36,37] eq 3 was successfully applied for estimation of H-bonded energies of the Cl$^-$···H−N bonds in crystals.[38]

The advantage of the above approaches is that they are applicable to bulk samples, and therefore, are able to deliver quantitative information about H-bonding in real ionic liquids (ILs). In contrast, various modeling techniques, applied to studies of ILs, dealt with separate ion pairs or their aggregates in the gas phase, or with larger but still limited-size ensembles of the counterions. Nevertheless, eqs 1−4, that are employed herein, are all of empirical character, and their reliability depends on the types of H-bonds to which they are applied. The most widely tested are applications of these relationships to evaluate the strength of H-bonding with the participation of hydroxyl groups. In case of ILs composed of 1-alkyl-3-methylimidazolium cations (e.g., 1-ethyl-3-methylimidazolium [C_2mim], Figure 1b) bearing three essentially acidic hydrogen

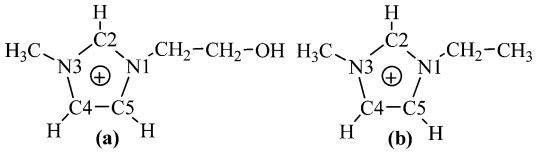

Figure 1. Atom numbering scheme for the 1-(2′-hydroxylethyl)-3-methylimidazolium [C_2OHmim] (a) and 1-ethyl-3-methylimidazolium [C_2mim] (b) cations.

atoms in the imidazolium ring, H-bonds are usually formed by the $C_{aromatic}$−H moieties of the cations. The applicability of eqs 1−4 to similar H-bonds in molecular liquids or solids is rather poorly studied. In addition, the changes to IR spectra induced by H-bonding interactions of imidazolium C−H moieties are often masked by Fermi resonances with overtones and combination of in-plane imidazolium ring modes.[20,39] For these reasons, ILs based on the 1-(2′-hydroxylethyl)-3-methylimidazolium cation ([C_2OHmim], Figure 1a) containing the hydroxyl functionality, were selected for study as this functionality can be used as a type of internal spectroscopic "probe" of H-bonding in the IL. The OH group can additionally act as an H-bond acceptor, providing much more varied types of H-bonding in comparison with nonfunctionalized ILs.

Previous studies focusing on H-bonding focus almost exclusively on 1,3-dialkylimidazolium salts as model systems. ILs with functional groups, often referred to as task-specific (TSILs),[40] may be used for specific applications,[41] and hydroxyl-functionalized ILs have been known since the introduction of the TSIL concept[42−44] and are used in catalytic processes[45,46] and other applications.[47] Despite growing interest in TSILs,[48,49] very little is known about their structural and spectroscopic features.[44,47,50] Detailed investigation of H-bonding in TSILs should lead to a better understanding of the cation/anion interactions and will further guide their systematic design.

The aim of this study was to obtain energetic characteristics of H-bonds in ILs formed between various anions and the [C_2OHmim]$^+$ cation. The following anions of various H-bond acceptor strengths, hexafluorophosphate [PF_6]$^-$, tetrafluoroborate [BF_4]$^-$, bis(trifluoromethanesulfonimide) [Tf_2N]$^-$, trifluoromethylsulfonate [OTf]$^-$, and trifluoroacetate [TFA]$^-$, were included in the study.

EXPERIMENTAL SECTION

The ILs 1-(2-hydroxylethyl)-3-methylimidazolium hexafluorophosphate [C_2OHmim][PF_6], tetrafluoroborate [C_2OHmim][BF_4], bis(trifluoromethanesulfonimide) [C_2OHmim][Tf_2N], trifluoromethylsulfonate [C_2OHmim][OTf], and trifluoroacetate [C_2OHmim][TFA] were prepared according to literature protocols.[42,43] Samples are dried under vacuum at 80 °C for 48 h prior to spectroscopic studies. Single crystals of [C_2OHmim][PF_6] suitable for X-ray diffraction analysis were obtained by slow cooling of a sample from 80 °C to room temperature over a period of 24 h.

dx.doi.org/10.1021/jp405255w | J. Phys. Chem. B 2013, 117, 9094−9105

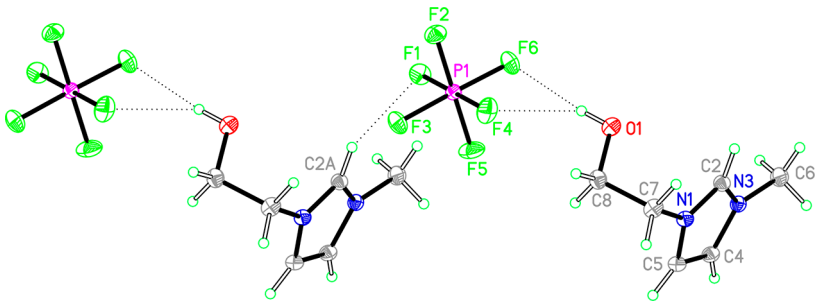

Figure 2. Structure of $[C_2OHmim][PF_6]$ in the solid state. Short contacts are shown with dashed lines. Selected bond lengths [Å] and angles [°]: N3−C2, 1.3312(10); N3−C4, 1.3822(9); N3−C6, 1.4713(9); N1−C2, 1.3388(9); N1−C5, 1.3862(9); N1−C7, 1.4692(10); C4−C5, 1.3623(10); C2−N3−C4, 108.93(6); C2−N3−C6, 124.70(6); C4−N3−C6, 126.37(6); C2−N1−C5, 108.42(6); C2−N1−C7, 125.04(6); C5−N1−C7, 126.12(6); N3−C2−N1, 108.72(6); O1−H1A···F4 (H···F, 2.40; O···F, 3.0376(10); <OHF, 133); O1−H1A···F6 (H···F, 2.29; O···F, 3.1176(9); <OHF, 169); C2A−H2A···F1 (H···F, 2.40; C···F, 3.2702(10); <CHF, 153).

X-ray Analysis. The diffraction data of $[C_2OHmim][PF_6]$ were measured at low temperature [100(2) K] using Mo K_α radiation on a Bruker APEX II CCD diffractometer equipped with a kappa geometry goniometer. The data set was reduced by EvalCCD[51] and then corrected for absorption.[52] The solution and refinement were performed by SHELX.[53] The crystal structure was refined using full-matrix least-squares based on F^2 with all non-hydrogen atoms anisotropically defined. Hydrogen atoms were placed in calculated positions by means of the "riding" model. More details can be found in Table 1S [Supporting Information (SI)].

Spectroscopic Methods. Raman spectra of solid and molten samples of $[C_2OHmim][PF_6]$ were recorded on a BRUKER RAM II module (using a Ge detector) attached to a BRUKER VERTEX 70 FTIR spectrometer in the range 10−4000 cm^{-1} with an optical resolution of 4 cm^{-1}. A Nd:YAG laser with a wavelength of 1064 nm and power of 500 mW was used as the excitation source. The sample was sealed in a standard glass capillary and cooled to 4 °C to afford a crystalline sample of $[C_2OHmim][PF_6]$. Heating of the capillary to slightly above 40 °C resulted in melting of the sample. The spectra of both crystalline and liquid $[C_2OHmim][PF_6]$ were registered at room temperature. Fourier transformed infrared (FTIR) spectra of samples were recorded using a Perkin-Elmer FT-IR Spectrum GX spectrometer. The spectrometer was flushed with dry nitrogen before and during the measurements. For each spectrum, 16 scans were obtained from 600 to 4000 cm^{-1}. Liquid samples were prepared as thin films between CaF_2 plates. The FTIR spectra were registered at the temperatures varying from −20 to +25 °C.

DFT Computations of the Gas-Phase Species. The "gas phase" calculations of isolated cations and anions, their ion pairs and small cluster-aggregates were carried out using the Gaussian 03 suite of programs.[54] For DFT, Becke's three-parameter exchange functional[55] was used in combination with the Lee−Yang−Parr correlation functional[56] (B3LYP) and standard 6-31G** basis set. All stationary points were characterized as minima by analysis of the Hessian matrices. The B3LYP functional is not able to account for van der Waals dispersion forces which contribute substantially to the weak intermolecular interactions.[57−60] Thus, dispersion-corrected energies were calculated (for B3LYP functional) within the recently developed approach DFT-D3[61] together with the Becke−Johnson (BJ) damping function.[62] For this purpose the program dftd3 v2.1 Rev1[63] was used. The obtained values, E_{disp}, were added to the electronic energies and the final energies were indicated as "$E+E_{disp}$". As shown recently, DFT-D3 performs very well in computations of interaction energies in ILs.[64] Dispersion corrections were not used in computations of IR spectra as these corrections have little influence on the IR spectra.[64−66]

Solid-State DFT Computations. In the CRYSTAL06 calculations[67] the B3LYP functional was used with the standard 6-31G** basis set. The default CRYSTAL06 options were used for the level of accuracy in evaluating the Coulomb and Hartree−Fock exchange series and a grid used in evaluating the DFT exchange-correlation contribution. Tolerance on energy controlling the self-consistent field convergence for geometry optimizations and frequencies computations was set to 10^{-8} and 10^{-9} Hartree, respectively. The number of points in the numerical first derivative calculation of the analytic nuclear gradients equals 2. The shrinking factor of the reciprocal space net was set to 3. Frequencies of normal modes were calculated within the harmonic approximation by numerical differentiation of the analytical gradient of the potential energy with respect to atomic position.[68] The IR intensities for normal modes were calculated from the dipole moment derivatives determined using well-localized Wannier functions of the unit cell to calculate the Born charge tensors.[68,69]

The obtained geometrical parameters were used in the computation of periodical electronic wave functions with the CRYSTAL98 program[70] at the B3LYP/6-31G** approximation level. The quantum-topological analysis of the crystalline electron density was performed with the TOPOND program.[71] Details of the electron-density topological analysis of molecular crystals are presented elsewhere.[72,73] The following electron-density features at the H···X (X = O and N) intermolecular bond critical point were considered: (i) the values of the electron density, ρ_b, (ii) its Laplasian, $\nabla^2\rho_b$, and (iii) the kinetic energy density, G_b. The first two values may be measured experimentally by means of the precise X-ray diffraction data, whereas G_b is used to estimate the energy of the particular H-bond or noncovalent interaction, see eq 4.

RESULTS

X-ray Structure of $[C_2OHmim][PF_6]$. The structure of $[C_2OHmim][PF_6]$ was determined by single crystal X-ray diffraction (Figure 2; Figures 1S and 2S, SI). The imidazolium cation has a typical planar conformation, and all of the ring C−C and C−N distances and angles are within the normal range for 1-alkyl-3-methylimidazolium cations.[74] The C−C bond of 2-hydroxylethyl moiety is almost perpendicular to the plane of

dx.doi.org/10.1021/jp405255w | J. Phys. Chem. B 2013, 117, 9094−9105

the heterocyclic ring, which is also typical for (N)CC fragments of alkylimidazolium crystal structures.[15,44,74] In contrast to the structure of 1-(2-hydroxypropyl)-3-methylimidazolium tetraphenylborate,[44] the $[C_2OHmim]^+$ cations do not form H-bonds with each other in the $[C_2OHmim][PF_6]$ crystal.

The crystal structure is characterized by multiple short contacts between the two counterions. Taking only the shortest contacts into account the crystal may be regarded as consisting of chains, in which each $[PF_6]^-$ anion is H-bonded to the OH group of one cation and the C2H moiety of another cation. Thus, each cation is H-bonded to two anions (Figure 2). Each hydroxyl group of the cation participates in two short OH···F contacts, the O···F6 distance (2.289 Å) is shorter than the O···F4 distance (2.405 Å), and the O−H···F6 angle (169.4°) is larger than the O−H···F4 angle (132.7°). Most probably, the OH···F6 contact represents an H-bond, whereas the OH···F4 contact should be regarded as a van der Waals interaction.

Electronic Structure, Vibrational Spectra, and Energy of the Hydrogen Bonds in the $[C_2OHmim][PF_6]$ Crystal. The space groups and unit cell parameters from the crystal were adopted with structural relaxations limited to the positional parameters of atoms. This approximation yields a reasonable description of various properties of molecular crystals and 3D periodical systems with H-bonds of different types and strengths.[75−83] The experimental values of the atomic positions were used as the starting point in the DFT computations with periodical boundary conditions. The structure was found to correspond to the minimum point on the potential energy surface. The mean deviation of the computed values of the O···O distances from the experimental ones is around 0.02 Å (Table 2S, SI). Relatively large deviations between experimental and computed distances are observed only for the PF_6···CH_2(O) contacts, see Table 2S.

The computed IR spectrum of the crystal (Figure 3a) is in reasonable agreement with the corresponding experimental spectrum (Figure 3b). According to the computations, the strongest IR band at ~3600 cm^{-1} in the high-frequency region is caused by the stretching vibrations of the hydroxyl group of the cation H-bonded with the closest $[PF_6]^-$ anion (νOH...$[PF_6]^-$). The second strongest feature in this region at 3174 cm^{-1} belongs to the stretching vibrations of C2−H group of the imidazolium ring H-bonded with another $[PF_6]^-$ anion (νC2H...$[PF_6]^-$). In-phase and out-of-phase stretchings of the C4−H and C5−H entities − ν_{ip}(C4,5)H and ν_{op}(C4,5)H − of the imidazolium ring give rise to a weaker band at ~3126 cm^{-1}. The band around 2900 cm^{-1} may be attributed to symmetrical stretching vibrations of CH_2(O) group.

Intermolecular (noncovalent) interactions in the crystal are characterized by $\nabla^2\rho_b > 0$ and $\rho_b < 0.02$ au (Tables 1 and 3S, SI) and, therefore, correspond to the case of the closed-shell atomic interactions.[84−86] The geometrical and electron density parameters of the strongest H-bonds in the $[C_2OHmim][PF_6]$ crystal are given in Table 1. The H-bond energies (E_{HB}) in the crystal, evaluated with eq 4, are equal to ~3 kcal·mol^{-1} and are therefore larger than the energies of the typical van-der-Waals interactions. The enthalpies ($-\Delta H_{HB}$) of the OH···F and C2H···F H-bonds in the $[C_2OHmim][PF_6]$ crystal were also estimated using eq 1. For this purpose the IR intensities have been calculated for isotope-isolated samples of the crystal (I) and the $[C_2OHmim]^+$ cation (I_0). For example, in the case of the C2H···F H-bond all hydrogen atoms except the (C2)H atom of the imidazolium ring were substituted by deuterium atoms. Such an approach results in $-\Delta H_{HB} \approx 2.8$ and 2.1 kcal·mol^{-1} for the OH···F and C2H···F H-bonds, respectively (Table 1). The estimated $-\Delta H_{HB}$ are in reasonable agreement with the corresponding E_{HB} values (Table 1), considering that these quantities are connected with each other by the relation $E_{HB} = -\Delta H_{HB} + 3RT/2$. Thus, at room temperature about 1 kcal·mol^{-1} should be added to the $-\Delta H_{HB}$ values in Table 1, producing E_{HB} values of ca. 3.8 and 3.1 kcal·mol^{-1} for the OH···F and CH···F bonds, respectively.

The computed value of the frequency shift of the OH stretching vibrations, $\Delta\nu$, equals to ~92 cm^{-1}. Such values are typical for the relatively weak H-bonds.[87,88] The enthalpy $-\Delta H_{HB}$ calculated for the OH···F H-bond via substitution of the red shift of $\Delta\nu$OH ≈ 92 cm^{-1} in the eq 2, amounts to ca. 2.4 kcal·mol^{-1}, which corresponds to $E_{HB} \approx 3.4$ kcal·mol^{-1} at room temperature. Thus, the estimates of the H-bonding strength in solid $[C_2OHmim][PF_6]$, obtained with the use of eqs 1, 2, and 4, are in excellent agreement.

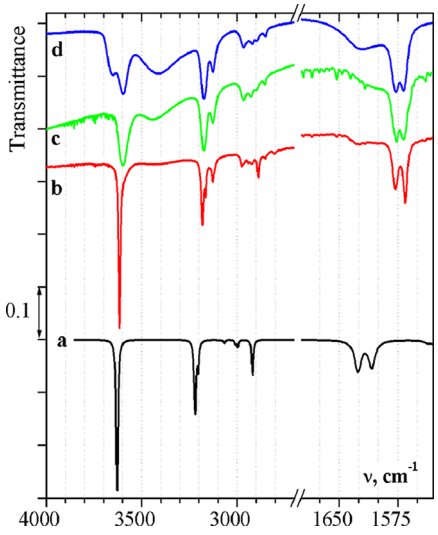

Figure 3. Computed (a) and experimental (b−d) IR spectra of the $[C_2OHmim][PF_6]$: a, solid-state DFT, the spectral range 4000−2750 cm^{-1} was scaled with a frequency scaling factor of 0.964;[94] b, crystal sample ($t \approx -20$ °C); c, liquid sample ($t \approx 25$ °C); d, liquid after absorption of atmospheric water.

Table 1. Values of the X···F Distances R(X···F) and Angles ∠X−H···F of the X−H···F Units, Where X = O or C, in the $[C_2OHmim][PF_6]$ Crystal: Experiment vs Solid-State DFT Computations (In Parentheses)[a]

	H-bonded fragment[a]	
	O1−H...F6	C2−H...F1
R(X···F), Å	3.118 (3.058)	3.270 (3.249)
∠X−H···F, deg	169.4 (169.5)	152.8 (151.3)
$-\Delta H_{HB}$,[b] kcal·mol^{-1}	2.8	2.1
ρ_b, a.u.	0.015	0.012
$\nabla^2\rho_b$, a.u.	0.049	0.044
E_{HB},[c] kcal·mol^{-1}	3.4	2.8

[a]The original numeration of atoms is taken from Figure 2. [b]Evaluated using eq 1. [c]Evaluated using eq 4 [a]The enthalpy of the H-bond, $-\Delta H_{HB}$, the electron density, ρ_b, its Laplasian, $\nabla^2\rho_b$, at the H-bond critical point, and the H-bond energy, E_{HB}, are given in the last four rows.

dx.doi.org/10.1021/jp405255w | J. Phys. Chem. B 2013, 117, 9094−9105

OH···F and OH···OH Hydrogen Bonding in Liquid [C_2OHmim][PF_6]. Various types of H-bonding interactions can be expected in the [C_2OHmim][PF_6] liquid as the crystal forces are no longer relevant. To delineate which of the possible H-bonds are formed in the liquid state IR (Figure 3) and Raman (Figure 3S, SI) spectra were recorded. The Raman spectrum of the liquid sample closely resembles the spectrum of the crystalline compound; in particular, no additional bands seem to appear, which suggests that there are no significant conformational changes of the [C_2OHmim]$^+$ cation.

A comparison of the IR spectra of the solid (Figure 3b) and liquid (Figure 3c) samples reveals that the νOH···[PF_6]$^-$ band at ca. 3600 cm^{-1} dominates the OH stretching vibration region in both spectra. Thus, OH···[PF_6]$^-$ H-bonds are formed both in solid and liquid [C_2OHmim][PF_6], and their strength is approximately the same in the both cases, as the positions of the νOH band in the spectra of the liquid and the solid samples coincide. The νOH band of methanol dissolved in liquid [C_4mim][PF_6] is observed at ~3618 cm^{-1}.[89] The same wavenumber was reported for the spectrum of methanol in a solution containing [PF_6]$^-$ anions in CH_2Cl_2.[90] A small red shift of νOH in the spectra of [C_2OHmim][PF_6] relative to the spectrum of methanol in [C_4mim][PF_6] suggests slightly stronger OH···[PF_6]$^-$ H-bonding in the former. It is not unreasonable to assume that this difference is due to the slightly stronger H-bonding basicity of [PF_6]$^-$ anions in [C_2OHmim]-[PF_6] relative to [C_4mim][PF_6], which is apparent from a comparison of the positions of the IR stretching (ν_1) and bending (ν_2) vibrations of water dissolved in both ILs.[91] In the spectrum [C_2OHmim][PF_6] containing water (Figure 3d), ν_1 (3653 cm^{-1}) is red-shifted, whereas ν_2 (1620 cm^{-1}) is blue-shifted, relative to 3672 and 1610 cm^{-1}, respectively, for water in [C_4mim][PF_6].[89] Thus, the H-bonds between water and the [PF_6]$^-$ anion are stronger in [C_2OHmim][PF_6] than in [C_4mim][PF_6].

The most important difference between the spectra of solid (Figure 3b) and liquid (Figure 3c) samples of [C_2OHmim]-[PF_6] is a broad band at ca. 3425 cm^{-1} observed only in the spectrum of the liquid. This feature may be assigned to νOH of the [C_2OHmim]$^+$ cation H-bonded to the hydroxyl groups of a neighboring cation that acts as an H-bond acceptor. For example, the bands at 3480−3525 cm^{-1} in the IR spectra of low-temperature argon matrices of methanol are assigned to a methanol H-bonded dimer, the bands in the range 3370−3430 cm^{-1} to a trimer, with the bands at lower wavenumbers apparently belonging to larger methanol aggregates.[92] Factor analysis of the IR spectra of methanol-hexane liquid mixtures demonstrates that the aggregates comprising more than two H-bonded methanol molecules absorb at wavenumbers lower than 3415 cm^{-1}.[93] In both cases the red shift of the νOH bands, belonging to the aggregates, relative to the νOH band of methanol free from H-bonding ($\Delta\nu$OH) amounts to ca. 250 cm^{-1}. This value corresponds well to the shift (ca. 265 cm^{-1}) of the band at ~3425 cm^{-1} in the spectra of the liquid (Figure 3c) relative to νOH = 3690 cm^{-1} computed for the isolated [C_2OHmim]$^+$ cation.[94] It should be noted that for liquid methanol, $\Delta\nu$OH exceeds 300 cm^{-1}, which suggests that OH···OH H-bonding in the [C_2OHmim][PF_6] IL is weaker than in the neat alcohol. Indeed, application of eq 2 to methanol produces $-\Delta H_{HB} \approx 5.3$ kcal·mol^{-1}, while the enthalpy of the OH···OH H-bond in the [C_2OHmim][PF_6] liquid, calculated with eq 2 amounts to ca. 5 kcal·mol^{-1}. The latter value, as well as the corresponding estimate of $E_{HB} \approx 6$ kcal·mol^{-1}, essentially exceed the values of $-\Delta H_{HB} \approx 2.4-2.8$ kcal·mol^{-1} or $E_{HB} \approx 3.4-3.8$ kcal·mol^{-1} obtained for OH···F H-bonds (Table 1).

IR Spectra and OH···[A]/OH···OH Hydrogen Bonding in [C_2OHmim][A] ILs (A = BF_4, Tf_2N, OTf, and TFA). H-bonds formed by the [C_2OHmim]$^+$ cation in ILs strongly depend on the counterion, as demonstrated by IR spectroscopy (Figure 4). The spectral shifts of the νOH bands belonging to the hydroxyl group of the [C_2OHmim]$^+$ cation, H-bonded to the anion, increase in the following order: [PF_6] < [BF_4] < [Tf_2N] ≪ [OTf] ≪ [TFA]. Application of eq 2 allows a comparison of the enthalpies of the H-bonds formed by the different anions (Table 2).

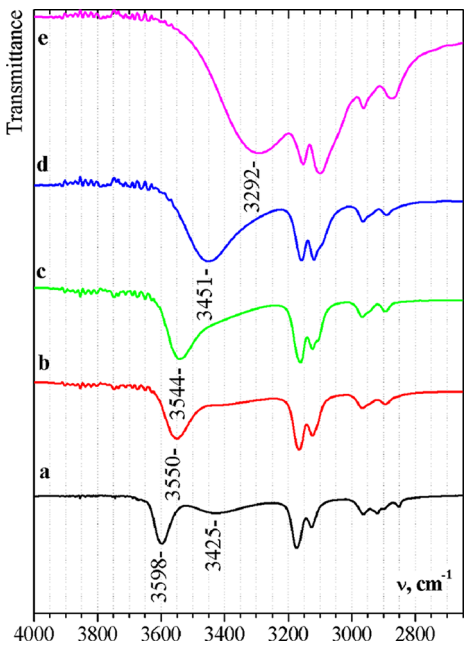

Figure 4. Experimental IR spectra in the range 4000−2700 cm^{-1}: a, [C_2OHmim][PF_6]; b, [C_2OHmim][BF_4]; c, [C_2OHmim][Tf_2N]; d, [C_2OHmim][OTf]; e, [C_2OHmim][TFA].

Table 2. Wavenumbers of νOH Bands, Their Red Shifts $\Delta\nu$OH[a] in the Spectra of Different ILs Based on the [C_2OHmim]$^+$ Cation, and the Enthalpies of H-Bonding $-\Delta H_{HB}$

anion	νOH, cm^{-1}	$\Delta\nu$OH, cm^{-1}	$-\Delta H_{HB}$, kcal·mol^{-1}
[PF_6]	3598	92	2.4
[BF_4]	3550	140	3.3
[Tf_2N]	3544	146	3.4
[OTf]	3451	239	4.7
[TFA]	3292	398	6.2

[a]Relative to νOH = 3690 cm^{-1} computed for the isolated [C_2OHmim]$^+$ cation.

The broad band at ca. 3425 cm^{-1}, assigned to νOH of H-bonded cationic clusters, is observed in the spectra of the ILs containing the [PF_6]$^-$, [BF_4]$^-$, and [Tf_2N]$^-$ anions (Figure 4a−c), though being much weaker for [C_2OHmim][BF_4] and [C_2OHmim][Tf_2N] than for [C_2OHmim][PF_6]. Thus, the hydroxyl group of the [C_2OHmim]$^+$ cation in the ILs is able to compete as an H-bond acceptor with the weakly coordinating [PF_6]$^-$, [BF_4]$^-$, and [Tf_2N]$^-$ anions. No clear features of

dx.doi.org/10.1021/jp405255w | J. Phys. Chem. B 2013, 117, 9094−9105

OH···OH bonding between the $[C_2OHmim]^+$ cations are observed in the spectra of $[C_2OHmim][OTf]$ and $[C_2OHmim][TFA]$.

C2H···[A] Hydrogen Bonding in $[C_2OHmim][A]$ ILs (A = PF_6, BF_4, Tf_2N, OTf, and TFA). Usually, the absorption at 3160 ± 15 cm^{-1} in the IR spectra of 1-alkyl-3-methylimidazolium based ILs, containing weakly coordinating anions such as $[PF_6]^-$, $[BF_4]^-$, and $[Tf_2N]^-$, is assigned to ν_{ip}(C4,5)H and ν_{op}(C4,5)H, and the feature at 3120 ± 15 cm^{-1} to νC2H.[39] It was also shown that both bands, being systematically complicated by Fermi resonances, have a C2H character.[20] According to solid state DFT computations described above νC2H vibrations give rise to a band at 3174 cm^{-1} in the IR spectrum of crystalline $[C_2OHmim][PF_6]$ (Figure 3b). A weaker band at 3126 cm^{-1} is assigned to in-phase and out-of-phase stretching of the C4−H and C5−H moieties of the imidazolium ring, ν_{ip}(C4,5)H and ν_{op}(C4,5)H. These assignments differ from previous assignments based on quantum chemical computations of isolated ion pairs or small aggregates of ion pairs (e.g., refs 18, 19, and 23 and references cited herein), since these "gas-phase" models do not take into account multiple secondary interactions present in crystals. In particular, it is proposed[95] that the anion on "top" of the imidazolium cation causes a blue shift of νCH frequencies relative to the isolated cation instead of a red shift. Our computations of isolated ion pairs (Figure 5) or an aggregate of three ion pairs (Figure 4S, SI) demonstrate that when the $[PF_6]^-$ anion approaches the "top" and/or "bottom" of the imidazolium ring a blue shift of νC2H and $\nu_{ip/op}$(C4,5)H amounting to 38 cm^{-1} takes place. The solid state DFT computations predict for both νC2H and $\nu_{ip/op}$(C4,5)H in $[C_2OHmim][PF_6]$ a blue shift of ca. 20−25 cm^{-1} relative to the isolated cation as a result of these multiple secondary interactions. Thus, two factors appear to influence the stretching frequencies of the CH groups of the imidazolium ring, CH···[A] H-bonds cause a red shift, whereas other secondary interactions can result in a blue-shift. When the H-bonding is weak, as in the case of $[C_2OHmim][PF_6]$, the net effect is a blue shift of νCH bands, whereas a red shift should be expected if stronger H-bonds are formed.[96]

The above effects as well as the effects of the Fermi resonance[20,39] can easily result in misinterpretation of the high frequency range of experimental IR spectra of ILs. To avoid possible misassignments of νC2−H and $\nu_{ip/op}$(C4,5)H bands in the IR spectra (Figure 4) of the studied ILs both types of vibrations can be designated as $\nu C_{aromatic}H$. The wavenumbers of $\nu C_{aromatic}H$ decrease (Table 3) as the νOH wavenumbers decrease (Table 2). Simultaneously, these bands become broader and stronger as the basicity of the anion increases. The intensity of lower-frequency $\nu C_{aromatic}H$ bands (at ca. 3100−3130 cm^{-1}) grows relative to the higher-frequency $\nu C_{aromatic}H$ bands (at ca. 3150−3170 cm^{-1}) in the spectra of ILs containing stronger H-bond acceptors (Figure 4, from bottom to top). Probably, the (C2)H hydrogen atom of the ring, which has a more acidic character than the other ring hydrogen atoms (C4)H and (C5)H, experiences the greatest H-bonding, causing a more pronounced red shift, growth of intensity and broadening of the νC2−H bands relative to the $\nu_{ip/op}$(C4,5)H components of complex $\nu C_{aromatic}H$ features. As a result, νC2−H and $\nu_{ip/op}$(C4,5)H bands in the spectrum of $[C_2OHmim][TFA]$ (Figure 4e), probably, interchange relative to the spectrum of $[C_2OHmim][PF_6]$ (Figure 4a), although this interpretation should be taken with caution.

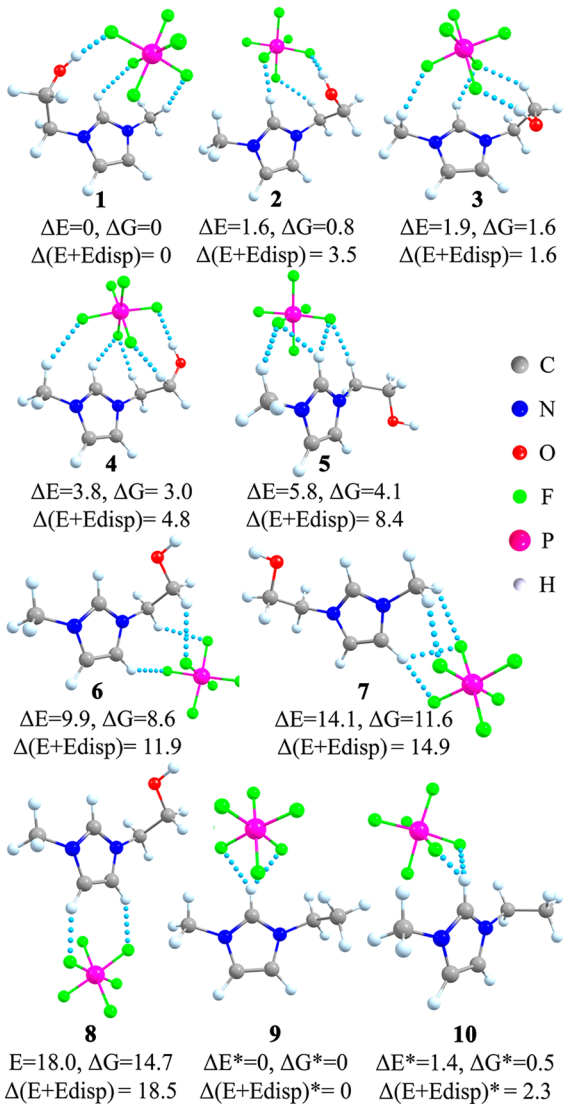

Figure 5. Optimized structures of ion pairs of $[C_2OHmim][PF_6]$ (**1**−**8**) and $[C_2mim][PF_6]$ (**9**−**10**), their electronic energies, (ΔE), Gibbs free energies (ΔG), and dispersion-corrected energies Δ(E + Edisp) relative to the global minimum structure **1** and **9**, respectively, in kcal·mol^{-1}. Relative energies of **9** and **10** are marked with *. Short contacts between F and H atoms are indicated with dotted lines.

Table 3. Wavenumbers of the $\nu C_{aromatic}H$ Bands in the Spectra of ILs with the $[C_2OHmim]^+$ Cation, and the Enthalpies $-\Delta H$ of (C2)H···[Anion] H-Bonding Estimated for the Corresponding Computed Isolated Ion Pairs with the Use of eq 1

anion	$\nu C_{aromatic}H$, cm^{-1}	$-\Delta H$, kcal·mol^{-1}
$[PF_6]$	3126, 3174	1.7−4.3
$[BF_4]$	3123, 3166	2.9−4.4
$[Tf_2N]$	3123/3107 sh, 3161	3.2−6.3
[OTf]	3119/3098 sh, 3158	4.6−5.4
[TFA]	3099 br, 3153	10

As the use of spectroscopic indicators of C2H...[A] H-bonding in quantum-chemically simulated "gas-phase" IR spectra is free from all the above-mentioned difficulties, the enthalpy of C2−H···[A] hydrogen bonds for B3LYP/6-31G** optimized isolated ion pairs, $[C_2OHmim][A]$, was estimated.

dx.doi.org/10.1021/jp405255w | J. Phys. Chem. B 2013, 117, 9094−9105

For this purpose the computed IR intensities for the localized, uncoupled stretching vibrations of the C2−H bond in the $[C_2OHmim][A]$ ion pair (I) and in the isolated $[C_2OHmim]^+$ cation (I_0) were substituted in eq 1. The applicability of eq 1 to different types of C−H···Y hydrogen bonds has been demonstrated elsewhere[25] on a limited number of examples, where experimental IR intensities of νC−H bands were measured. The computed $-\Delta H$ values are listed in Table 3. Intervals of the $-\Delta H$ estimates are given for the $[C_2OHmim][A]$ ILs (A = PF_6, BF_4, Tf_2N, and OTf), as several ion pairs with different strengths of C2H...[A] H-bonding were optimized for each IL (Figure 5; Figures 6S and 7S, SI). The resulting values of $-\Delta H \approx 2 - 4$ kcal·mol^{-1} for the $[C_2OHmim][PF_6]$ ion pairs compare well with the enthalpy of H-bonding ($-\Delta H \approx 2.1$ kcal·mol^{-1}) obtained for solid $[C_2OHmim][PF_6]$ from eq 4, considering that the H-bonding in the crystal is weaker than in isolated ion pairs because of anticooperativity effects acting in the bulk IL.[22,23,97] The interval of 3.2−6.3 kcal·mol^{-1} obtained for the $[C_2OHmim][Tf_2N]$ ion pairs is in reasonable agreement with published[98] estimates of C2H···$[Tf_2N]$ H-bonds, ca. 5 kcal·mol^{-1}, based on HF/3-21G computations of binding energies for clusters of $[C_2mim][Tf_2N]$ ion pairs and the application of approaches similar to the techniques described below. Overall, the intervals of $-\Delta H$ estimates for the different anions in Table 3, although partially overlapping, follow the experimentally observed trend based on the $\nu C_{aromatic}H$ wavenumbers, which, in turn, parallel the trend in red shifts of the νOH wavenumbers (Table 2), i.e., $[PF_6] < [BF_4] < [Tf_2N] < [OTf] \ll [TFA]$.

Possible Structures of Counterions and Their Associations in the Gas Phase. As described above, the H-bonds in crystals of $[C_2OHmim][PF_6]$ are formed by the OH and C2H groups (H-donors) and the fluorine atoms of the $[PF_6]^-$ anion (H-acceptors). In the liquid state conformational flexibility of both the $[C_2OHmim]^+$ cation and various ion pairs, as well as the formation of different types of H-bonds can be anticipated. In particular, as was shown above, the OH groups of the $[C_2OHmim]^+$ cation in several of the ILs can H-bond to the hydroxyl groups of the neighboring cations, acting as H-acceptors instead of the anion.

However, to better understand the structure and H-bonding in the liquid phase of the ILs various conformers and ion associations were analyzed using quantum chemical "gas-phase" computations. Possible conformations of the $[C_2OHmim]^+$ cation are presented in Figure 5S (SI). The conformation of the hydroxylethyl group of the cation is determined by the torsion angles, τ_1 = N1−C−C−O and τ_2 = C−C−O−H, which can be equal to *ca.* 180° in the anti-conformation or ca. ± 60° in the ± gauche-conformation. The computations suggest that the gauche-conformation about the (N1)C−C(O) bond observed in the crystal of $[C_2OHmim][PF_6]$ is strongly energetically preferable relative to the anti-conformation ($\Delta E \approx \Delta G \approx 5$ kcal·mol^{-1}), whereas the energy gaps between ± gauche- and anti-conformations about the (C)C−O(H) bond do not exceed 1 kcal·mol^{-1} (Figure 5S).

Both gauche,gauche- and gauche,anti-conformers are present in the optimized structures of $[C_2OHmim][PF_6]$ ion pairs (Figure 5).[99] The most stable ion pair, **1**, is obtained after optimization of the starting geometry taken from the X-ray structure. As a result of the optimization the anion closely approaches the top of the imidazolium ring and adopts a position not found in the crystal (Figure 5, **1**). It should be noted that the three other most stable ion pairs, **2**−**4**, (Figure 5) do not completely correspond to the X-ray experiment either.

In all three ion pairs the anion forms H-bonds via the OH and C2H groups of the same cation, whereas in the crystal each $[PF_6]^-$ anion is H-bonded to the OH group of one cation and the C2H group of another cation (Figure 2). The latter type of C2H···$[PF_6]^-$ H-bond is represented in ion pair **5**, corresponding to this fragment of the experimental structure of the $[C_2OHmim][PF_6]$ crystal. The other short contacts found in the crystal are reasonably well reproduced in the optimized ion pairs **6** and **7**.

The deviations of the structures computed in the gas phase from the crystal structure are unlikely to be due to deficiencies of the DFT method as the same level of theory applied to the periodical electronic wave functions analysis successfully reproduced the experimental structural parameters. Apparently, multiple secondary interactions, which were ignored in the computations of the ion pairs discussed above, strongly influence the mode of association of the counterions. The situation is only slightly improved if clusters of ion pairs are computed. In particular, a fragment of the crystal structure containing three ion pairs (Figure 2) coils up during the optimization (Figure 4S, SI).

Optimized structures of the $[C_2OHmim][BF_4]$ ion pairs (Figure 6S, SI) and their relative energies are very similar to those in Figure 5. Some representative optimized structures of $[C_2OHmim][A]$ ion pairs, where A = $[Tf_2N]$, [OTf], or [TFA], are shown in Figure 7S (SI). Short contacts of type CH···F are present in the majority of the computed ion pairs. According to the computations, the short contacts of the hydrogen atoms of the imidazolium ring not only induce a red shift of the corresponding νCH bands but also a substantial growth in their intensity, which is regarded as the most reliable marker of H-bond formation.[25] These effects are practically negligible for the CH bonds of alkyl groups, indicating that these hydrogen atoms are not involved in H-bonding.

According to the computational analysis two types of H-bonds absent in crystalline $[C_2OHmim][PF_6]$ are possible in gas or liquid states. First, the OH groups of neighboring cations can be H-bonded to each other (Figure 6a), and second, H-bonds could be formed by one of the ring hydrogen atoms

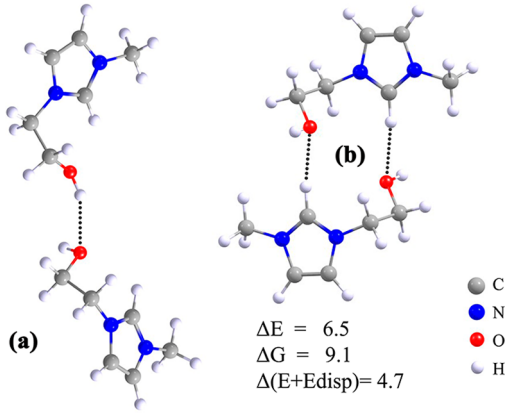

Figure 6. Optimized structures of the H-bonded dimers of $[C_2OHmim]^+$ cations. Short contacts between the O and H atoms are indicated with dotted lines. Electronic (ΔE), Gibbs free energies (ΔG), and dispersion-corrected energies Δ(E + Edisp) of b relative to the structure a are shown, in kcal·mol^{-1}.

dx.doi.org/10.1021/jp405255w | J. Phys. Chem. B 2013, 117, 9094−9105

acting as the H-donor and the OH group of the neighboring cation as the H-acceptor (Figure 6b). Dimers of H-bonded cations, similar to that shown in Figure 6b, were found in crystals of 1-(2-hydroxypropyl)-3-methylimidazolium tetraphenylborate.[44]

The simulated IR spectrum of the dimer shown in Figure 6b is characterized by a negligibly small red shift, $\Delta\nu$OH, relative to the νOH frequency of the isolated cation, which does not correspond to the experimentally determined spectra of the compounds. Thus, this type of dimer is not formed in detectable amounts in the ILs. The red shift, $\Delta\nu$OH = 93 cm^{-1}, computed for the dimer shown in Figure 6a is also smaller than the experimental value, amounting to ca. 265 cm^{-1}. $\Delta\nu$OH computed for the corresponding trimer (183 cm^{-1}) or tetramer (ca. 220 cm^{-1}) of the H-bonded cations (Figure 8S, SI) match the experimental values much better, thus providing further support to the empirical assignment of the IR band at ca. 3425 cm^{-1} in the recorded spectra to νOH of cationic aggregates comprising at least three H-bonded entities.

A comparison of the computed binding energies (BE) of the ion pairs shown in Figure 5 allows the strength of the OH···F hydrogen bonds between the $[C_2OHmim]^+$ cation and the $[PF_6]^-$ anion to be estimated in the gas phase. For example, ion pairs **2**–**4** are bound by both C2H···F and OH···F H-bonds, whereas in ion pair **5**, which has a similar structure, the OH···F H-bond is absent. Assuming that the energy of C2H···F H-bonding ($E_{C2H\cdots F}$) is the same for ion pairs **2**–**5**, then $E_{OH\cdots F}$ can be roughly estimated as the difference between the BEs of ion pairs **2** and **5**, **3** and **5**, and **4** and **5**. If the dispersion correction is taken into account, such an approach produces $E_{OH\cdots F}$ of ca. 5, 7, and 4 kcal·mol^{-1}, respectively, with a mean value of ca. 5 ± 2 kcal·mol^{-1}.

The strength of OH···F hydrogen bonding can also be evaluated on the basis of a similar comparison of BE for ion pairs **2** or **3**, bound by both C2H···F and OH···F H-bonds, and the similar ion pair, **9** (Figure 5), where only the C2H···F bond is formed (a validation of this approach is provided in the SI). Such an approach results in an estimate of $E_{OH\cdots F} \approx 4 \pm 2$ kcal·mol^{-1}.

The energy of OH···F H-bond in $[C_2OHmim][PF_6]$ ion pairs was also estimated using the empirical eqs 1 and 2. For this purpose the IR intensities and frequencies, respectively, of the νOH vibrations calculated for the ion pair and for the isolated $[C_2OHmim]^+$ cation were compared. Such an approach, applied to ion pair **1** (Figure 5), resulted in $-\Delta H \approx 4.2$ and 4.1 kcal·mol^{-1} (or $E_{HB} \approx 5.2$ and 5.1 kcal·mol^{-1}) for eqs 1 and 2, respectively.

Thus, different approximations, based on computations of isolated ion pairs, allow estimates of $E_{OH\cdots F}$ to be obtained, which agree reasonably well with the estimates of $E_{OH\cdots F} \approx 3.4 - 3.8$ kcal·mol^{-1} based on analysis of periodic wave function of crystalline $[C_2OHmim][PF_6]$ and application of eqs 1 and 4. As expected, H-bonding in the crystal is less strong than in the isolated ion pairs because of anticooperativity effects acting in the bulk IL.[22,23,97,100]

DISCUSSION

Attaching the hydroxyl group to the imidazolium cation of an IL provided an internal spectroscopic "probe" that allows the H-bonding in the bulk ILs to be assessed. Analysis of such a convenient spectroscopic indicator for H-bonding, i.e., the νOH band in the IR spectra of crystalline and molten samples of $[C_2OHmim][PF_6]$, demonstrates that OH···$[PF_6]$ H-bonds of approximately the same strength are present in both the solid and liquid states. An additional feature characterizing H-bonding in liquid $[C_2OHmim][PF_6]$ comprises the formation of aggregates of self-associated $[C_2OHmim]^+$ cations including probably at least three or four species H-bonded between each other by OH···OH H-bonds.

The energy of the OH···$[PF_6]$ H-bond (E_{HB}) in liquid $[C_2OHmim][PF_6]$ was estimated using two main approaches, First, a theoretical analysis of the solid-state electron-density using eq 4. Second, analysis of spectroscopic features of H-bond formation such as red-shift of νOH vibrational frequency with eq 2, or a growth of the corresponding IR intensity with eq 1. Both approaches produce almost the same value of $E_{HB} \approx 3.4 - 3.8$ kcal·mol^{-1}, representing the first quantitative estimate of the strength of H-bonding in a bulk IL. Only eq 2 could be applied to the analysis of OH···OH bonds in liquid $[C_2OHmim][PF_6]$, producing the E_{HB} estimate of ca. 6 kcal·mol^{-1}. The corresponding enthalpies of OH···$[PF_6]^-$ and OH···OH H-bonds amounted to 2.4 and 5 kcal·mol^{-1}, respectively. Both the energetic and spectroscopic characteristics of H-bonds formed by the hydroxyl group of the cation in the IL are similar to the corresponding parameters of OH···$[PF_6]^-$ and OH···OH H-bonds formed by methanol dissolved in $[C_4mim][PF_6]$ and in neat methanol, respectively.

Both types of H-bonding were found also in other ILs containing the weakly coordinating anions $[BF_4]^-$ and $[Tf_2N]^-$. No clear manifestations of OH···OH self-association of the cations were found in the IR spectra of ILs comprising more basic anions, i.e., $[OTf]^-$ and $[TFA]^-$. Equation 2 was used to estimate the enthalpies of the H-bonds ($-\Delta H$) formed by the hydroxyl group of the $[C_2OHmim]^+$ cation with different anions. The $-\Delta H$ values grow in the following order: $[PF_6]^-$ (2.4 kcal·mol^{-1}) < $[BF_4]^-$ (3.3 kcal·mol^{-1}) < $[Tf_2N]^-$ (3.4 kcal·mol^{-1}) < $[OTf]^-$ (4.7 kcal·mol^{-1}) < $[TFA]^-$ (6.2 kcal·mol^{-1}).

It should be noted, that the H-bonds in ionic liquids were studied with NMR techniques, e.g., refs. cited in.[21] These studies showed the existence of the extended H-bonded network, however, the accuracy of the experimental data was insufficient for a quantitative description of the particular H-bond. One can expect that the targeted experiments can evaluate the change in proton chemical shift,[101] and identify the effect of the electron density distribution caused by the H-bond formation on the chemical shifts of ^{15}N and ^{19}F.[102]

Hydrogen bonds of different strength were detected in the classical molecular dynamics simulations[103,104] and combined molecular mechanical/quantum mechanical studies[105] of imidazolium-based ionic liquids. Their quantitative description implies introduction of thermal fluctuations and quantization of proton motion, e.g., see ref 106.

The first estimate of the strength of H-bonds formed in bulk ILs between an anion with the aromatic proton of an imidazolium cation was obtained from an analysis of the periodical electronic wave functions of the $[C_2OHmim][PF_6]$ crystal. Application of eqs 1 and 4 produced an estimate of $E_{HB} \approx 2.8 - 3.1$ kcal·mol^{-1} for the C2H···$[PF_6]^-$ bond. This value is in reasonable agreement with estimates of $-\Delta H \approx 2$–4 kcal·mol^{-1} obtained for C2H...$[PF_6]$ H-bonds using eq 1 on the basis of IR intensities computed for various "gas-phase" optimized $[C_2OHmim][PF_6]$ ion pairs. The intervals of similar "gas-phase" $-\Delta H$ estimates, obtained for C2H H-bonds with different anions follow the experimentally observed trend, based on $\nu C_{aromatic}H$ wavenumbers which, in turn, parallel the

dx.doi.org/10.1021/jp405255w | J. Phys. Chem. B 2013, 117, 9094–9105

trend in red shifts of νOH wavenumbers: $[PF_6]^-$ < $[BF_4]^-$ < $[Tf_2N]^-$ < $[OTf]^-$ ≪ $[TFA]^-$.

It should be noted, however, that any comparison between isolated ion pairs and bulk ILs should be taken with caution, and this study clearly demonstrates the importance of multiple secondary interactions functioning in bulk ILs. These interactions, even being much weaker than interionic interactions within isolated ion pair, nevertheless influence the structure and vibrational spectra of ILs. Thus, such models as the isolated ion pairs or clusters of ion pairs cannot reproduce/predict the above-mentioned characteristics of bulk ILs in detail. Indeed, neither the optimized ion pairs, nor the clusters of ion pairs reproduce the X-ray experimental structure of $[C_2OHmim][PF_6]$. The deviations of the structures computed in the gas phase from the crystal structure are not due to deficiencies in the DFT method, as the same level of theory applied to the periodical electronic wave functions analysis successfully reproduced the experimental geometry.

Multiple secondary interactions, ignored in the computations of the ion pairs, strongly influence the stretching frequencies of the imidazolium ring CH groups. Surprisingly, in the $[C_2OHmim][PF_6]$ crystal these interactions even cause a blue shift of the $\nu C_{aromatic}H$ bands in spite of the CH···$[PF_6]^-$ H-bonds. According to the "gas-phase" computations of ion pairs or ion aggregates, $\nu C_{aromatic}H$ bands should undergo a red shift due to the effect of these H-bonds.

The strength of H-bonding interactions in the ILs was also found to be influenced by secondary interactions. Using various approximations it was possible to estimate the energy of OH···$[PF_6]^-$ H-bonds, both in ion pairs isolated in gas phase ($E_{HB} \leq 7$ kcal·mol^{-1}), and in the bulk IL ($E_{HB} \approx 3.4$ −3.8 kcal·mol^{-1}). A comparison of these two values demonstrates that H-bonding in the crystal is weaker than in isolated ion pairs, apparently due to anticooperativity effects. All previous discussions of anticooperativity in IL were based on comparisons of spectroscopic or geometrical parameters of isolated ion pairs and clusters of ion pairs computed in gas phase quantum-chemically.[22,23,97,100] The general conclusion from these studies was that H-bonding in isolated ion pairs is stronger than in clusters. The quantitative data on E_{HB} described herein indicates that the effects of anticooperativity in bulk ILs may amount to *ca.* 50% of the entire value.

CONCLUSIONS

Quantum-chemical modeling of bulk ILs in combination with experimental structural and spectroscopic methods has delivered the first quantitative characteristics of the strength of H-bonding in actual ILs. Various empirical approaches, used to obtain these characteristics, give rise to practically coinciding estimates of energy or enthalpy of the H-bonds. Notably, a comparison of these data with the corresponding values obtained on the basis of quantum-chemical "gas-phase" computations has revealed both analogies and disparities between structural, spectroscopic and energetic characteristics of H-bonding between ionic components of ILs in the gas and condensed phases. This disparity suggests that an analysis of the role of H-bonding in ILs based solely on "gas-phase" computations can lead to the misinterpretation of data. The quantitative analysis described herein should facilitate further studies on the role of hydrogen bonding in ILs and ultimately it could aid the rational design of ILs with specific physical and chemical properties.

ASSOCIATED CONTENT

Supporting Information

Crystal data from X-ray and computations, Raman spectra, and details of computations. This material is available free of charge via the Internet at http://pubs.acs.org.

AUTHOR INFORMATION

Corresponding Author

*E-mail: skatsyuba@yahoo.com; katsyuba@iopc.ru (S.A.K.). E-mail: paul.dyson@epfl.ch (P.J.D.).

Notes

The authors declare no competing financial interest.

ACKNOWLEDGMENTS

Financial support from the EPFL, the Switzerland-Russia S&T Cooperation Program and the Swiss National Science Foundation (Utilisation of specific infrastructure grant) are gratefully acknowledged. M.V.V. and E.E.Z. thank Russian Foundation for Basic Research (Grants 11-03-00583 and 12-03-31214_mol-a, respectively) for partial financial support of this study. M.V.V. thanks Drs. Ilya G. Shenderovich and Ruslan E. Asfin for useful discussions.

REFERENCES

(1) Wasserscheid, P.; Keim, W. Ionic Liquids - New 'Solutions' for Transition Metal Catalysis. *Angew. Chem., Int. Ed.* **2000**, *39*, 3772−3789.

(2) Dong, K.; Zhang, S. Hydrogen Bonds: A Structural Insight into Ionic Liquids. *Chem.—Eur. J.* **2012**, *18*, 2748−2761.

(3) Fumino, K.; Peppel, T.; Geppert-Rybczynska, M.; Zaitsau, D. H.; Lehman, J. K.; Verevkin, S. P.; Köckerling, M.; Ludwig, R. The Influence of Hydrogen Bonding on the Physical Properties of Ionic Liquids. *Phys. Chem. Chem. Phys.* **2011**, *13*, 14064−14075.

(4) Hallett, J. P.; Welton, T. Room-Temperature Ionic Liquids: Solvents for Synthesis and Catalysis. 2. *Chem. Rev.* **2011**, *111*, 3508−3576.

(5) Dong, K.; Song, Y.; Liu, X.; Cheng, W.; Yao, X.; Zhang, S. Understanding Structures and Hydrogen Bonds of Ionic Liquids at the Electronic Level. *J. Phys. Chem. B* **2012**, *116*, 1007−1017.

(6) Skarmoutsos, I.; Dellis, D.; Matthews, R. P.; Welton, T.; Hunt, P. A. Hydrogen Bonding in 1-Butyl- and 1-Ethyl-3-Methylimidazolium Chloride Ionic Liquids. *J. Phys. Chem. B* **2012**, *116*, 4921−4933.

(7) Zhang, Y.; Maginn, E. J. The Effect of C2 Substitution on Melting Point and Liquid Phase Dynamics of Imidazolium Based-Ionic Liquids: Insights from Molecular Dynamics Simulations. *Phys. Chem. Chem. Phys.* **2012**, *14*, 12157−12164.

(8) Dupont, J. On the Solid, Liquid and Solution Structural Organization of Imidazolium Ionic Liquids. *J. Braz. Chem. Soc.* **2004**, *15*, 341−350.

(9) Fumino, K.; Reichert, E.; Wittler, K.; Hempelmann, R.; Ludwig, R. Low-Frequency Vibrational Modes of Protic Molten Salts and Ionic Liquids: Detecting and Quantifying Hydrogen Bonds. *Angew. Chem., Int. Ed.* **2012**, *51*, 6236−6240.

(10) Crowhurst, L.; Mawdsley, P. R.; Perez-Arlandis, J. M.; Salter, P. A.; Welton, T. Solvent-Solute Interactions in Ionic Liquids. *Phys. Chem. Chem. Phys.* **2003**, *5*, 2790−2794.

(11) Weingärtner, H. Understanding Ionic Liquids at the Molecular Level: Facts, Problems, and Controversies. *Angew. Chem., Int. Ed.* **2008**, *47*, 654−670.

(12) Tsuzuki, S.; Tokuda, H.; Mikami, M. Theoretical Analysis of the Hydrogen Bond of Imidazolium C2-H with Anions. *Phys. Chem. Chem. Phys.* **2007**, *9*, 4780−4784.

(13) Schröder, C.; Rudas, T.; Steinhauser, O. Simulation Studies of Ionic Liquids: Orientational Correlations and Static Dielectric Properties. *J. Chem. Phys.* **2006**, *125*, 244506.

(14) Zhao, W.; Leroy, F.; Heggen, B.; Zahn, S.; Kirchner, B.; Balasubramanian, S.; Muller-Plathe, F. Are There Stable Ion-Pairs in Room-Temperature Ionic Liquids? Molecular Dynamics Simulations of 1-N-Butyl-3-Methylimidazolium Hexafluorophosphate. *J. Am. Chem. Soc.* **2009**, *131*, 15825−15883.
(15) Dieter, K. M.; Dymek, C. M., Jr.; Heimer, N. E.; Rowang, J. W.; Wilkes, J. S. Ionic Structure and Interactions in 1-Methyl-3-Ethylimidazolium Chloride-Alcl3Molten Salts. *J. Am. Chem. Soc.* **1988**, *110*, 2722−2726.
(16) Dymek, C. M., Jr.; Grossie, D. A.; Fratini, A. V.; Adams, W. W. Evidence for the Presence of Hydrogen-Bonded Ion-Ion Interactions in the Molten Salt Precursor, 1-Methyl-3-Ethylimidazolium Chloride. *J. Mol. Struct.* **1989**, *213*, 25−34.
(17) Elaiwi, A.; Hitchcock, P. B.; Seddon, K. R.; Srinivasan, N.; Tan, Y.-M.; Welton, T.; Zora, J. A. Hydrogen Bonding in Imidazolium Salts and its Implications for Ambient-Temperature Halogenoaluminate-(III) Ionic Liquids. *J. Chem. Soc., Dalton Trans.* **1995**, *21*, 3467−3472.
(18) Katsyuba, S. A.; Dyson, P. J.; Vandyukova, E. E.; Vidiš, A. Molecular Structure, Vibrational Spectra, and Hydrogen Bonding of the Ionic Liquid 1-Ethyl-3-Methyl-1H-Imidazolium Tetrafluoroborate. *Helv. Chim. Acta* **2004**, *87*, 2556−2565.
(19) Katsyuba, S. A.; Zvereva, E. E.; Vidiš, A.; Dyson, P. J. Application of Density Functional Theory and Vibrational Spectroscopy toward the Rational Design of Ionic Liquids. *J. Phys. Chem. A* **2007**, *111*, 352−370.
(20) Grondin, J.; Lassegues, J.-C.; Cavagnat, D.; Buffeteau, T.; Johansson, P.; Holomb, R. Revisited Vibrational Assignments of Imidazolium-Based Ionic Liquids. *J. Raman Spectrosc.* **2011**, *42*, 733−743.
(21) Katsyuba, S. A.; Griaznova, T. P.; Vidiš, A.; Dyson, P. J. Structural Studies of the Ionic Liquid 1-Ethyl-3-Methylimidazolium Tetrafluoroborate in Dichloromethane Using a Combined DFT-NMR Spectroscopic Approach. *J. Phys. Chem. B* **2009**, *113*, 5046−5051.
(22) Fei, Zh.; Ang, W. H.; Zhao, D.; Scopelliti, R.; Zvereva, E. E.; Katsyuba, S. A.; Dyson, P. J. Revisiting Ether-Derivatized Imidazolium-Based Ionic Liquids. *J. Phys. Chem. B* **2007**, *111*, 10095−10108.
(23) Köddermann, T.; Wertz, C.; Heintz, A.; Ludwig, R. Ion-Pair Formation in the Ionic Liquid 1-Ethyl-3-Methylimidazolium Bis-(Triflyl)Imide as a Function Of Temperature and Concentration. *Chem. Phys. Chem.* **2006**, *7*, 1944−1949.
(24) Fumino, K.; Wulf, A.; Ludwig, R. The Potential Role of Hydrogen Bonding in Aprotic and Protic Ionic Liquids. *Phys. Chem. Chem. Phys.* **2009**, *11*, 8790−8794.
(25) Iogansen, A. V. Direct Proportionality of the Hydrogen Bonding Energy and the Intensification of the Stretching N (XH) Vibration in Infrared Spectra. *Spectrochim. Acta, Part A* **1999**, *55*, 1585−1672.
(26) Purcell, K. F.; Drago, R. S. Theoretical Aspects of the Linear Enthalpy Wavenumber Shift Relation for Hydrogen-Bonded Phenols. *J. Am. Chem. Soc.* **1967**, *89*, 2874−2879.
(27) Bader, R. W. F. *Atoms in Molecules: A Quantum Theory*; Oxford University Press: New York, 1990.
(28) Tsirelson, V. G. In *The Quantum Theory of Atoms in Molecules: From Solid State to DNA and Drug Design*; Matta, C., Boyd, R., Eds.; Wiley-VCH: Weinheim, Germany, 2007; Chapter 10.
(29) Arunan, E.; Desiraju, G. R.; Klein, R. A.; Sadlej, J.; Scheiner, S.; Alkorta, I.; Clary, D. C.; Crabtree, R. H.; Dannenberg, J. J.; Hobza, P.; et al. Definition of the Hydrogen Bond (IUPAC Recommendations 2011). *Pure Appl. Chem.* **2011**, *83*, 1637−1641.
(30) Asfin, R. E.; Denisov, G. S.; Tokhadze, K. G. The Infrared Spectra and Enthalpies of Strongly Bound Dimers of Phosphinic Acids in the Gas Phase. $(CH_2Cl)_2POOH$ and $(C_6H_5)_2POOH$. *J. Mol. Struct.* **2002**, *608*, 161−168.
(31) Kong, S.; Shenderovich, I. G.; Vener, M. V. Density Functional Study of the Proton Transfer Effect on Vibrations of Strong (Short) Intermolecular O-H···N/O-···H-N+ Hydrogen Bonds in Aprotic Solvents. *J. Phys. Chem. A* **2010**, *114*, 2393−2399.
(32) Rozenberg, M.; Loewenschuss, A.; Marcus, Y. An Empirical Correlation Between Stretching Vibration Redshift and Hydrogen Bond Length. *Phys. Chem. Chem. Phys.* **2000**, *2*, 2699−2702.
(33) Rozenberg, M.; Shoham, G.; Reva, I.; Fausto, R. A Correlation between the Proton Stretching Vibration Red Shift and the Hydrogen Bond Length in Polycrystalline Adesnosine and Uridine. *Phys. Chem. Chem. Phys.* **2005**, *7*, 2376−2383.
(34) Espinosa, E.; Molins, E.; Lecomte, C. Hydrogen Bond Strengths Revealed by Topological Analyses of Experimentally Observed Electron Densities. *Chem. Phys. Lett.* **1998**, *285*, 170−173.
(35) Mata, I.; Alkorta, I.; Espinosa, E.; Molins, E. Relationships between Interaction Energy, Intermolecular Distance and Electron Density Properties in Hydrogen Bonded Complexes under External Electric Fields. *Chem. Phys. Lett.* **2011**, *507*, 185−189.
(36) Vener, M. V.; Egorova, A. N.; Churakov, A. V.; Tsirelson, V. G. Intermolecular Hydrogen Bond Energies in Crystals Evaluated Using Electron Density Properties: DFT Computations with Periodic Boundary Conditions. *J. Comput. Chem.* **2012**, *33*, 2303−2309.
(37) Shishkina, A. V.; Zhurov, V. V.; Stash, A. I.; Vener, M. V.; Pinkerton, A. A.; Tsirelson, V. G. Noncovalent Interactions in Crystalline Picolinic Acid N-Oxide: Insights from Experimental and Theoretical Charge Density Analysis. *Cryst. Growth Des.* **2013**, *13*, 816−828.
(38) Nelyubina, Y. V.; Antipin, M.Yu.; Lyssenko, K. A. *J. Phys. Chem. A* **2007**, *111*, 1091−1095.
(39) Lassegues, J.-C.; Grondin, J.; Cavagnat, D.; Johansson, P. New Interpretation of the CH Stretching Vibrations in Imidazolium-Based Ionic Liquids. *J. Phys. Chem. A* **2009**, *113*, 6419−6421.
(40) Visser, A. E.; Swatloski, R. P.; Reichert, W. M.; Mayton, R.; Sheff, S.; Wierzbicki, A.; Davis, J. H., Jr.; Rogers, R. D. Task-Specific Ionic Liquids for the Extraction of Metal Ions from Aqueous Solutions. *Chem. Commun.* **2001**, 135−136.
(41) Fei, Z.; Dyson, P. J. The Making of Liquids-The Chemist's Equivalent of the Iphone. *Chem. Commun.* **2013**, *49*, 2594−2596.
(42) Branco, L. C.; Rosa, J. N.; Ramos, J. J. M.; Afonso, C. A. M. Preparation and Characterization of New Room Temperature Ionic Liquids. *Chem.—Eur. J.* **2002**, *8*, 3671−3677.
(43) Najdanovic-Visak, V.; Rodriguez, A.; Visak, Z. P.; Rosa, J. N.; Afonso, C. A. M.; da Ponte, M. N.; Rebelo, L. P. N. Co-Solvent Effects in LLE Of 1-Hydroxyethyl-3-Methylimidazolium Based Ionic Liquids + 2-Propanol + Dichloromethane or 1,2-Dichloroethane. *Fluid Phase Equilib.* **2007**, *254*, 35−3841.
(44) Holbrey, J. D.; Turner, M. B.; Reichert, W. M.; Rogers, R. D. New Ionic Liquids Containing an Appended Hydroxyl Functionality from the Atom-Efficient, One-Pot Reaction of 1-Methylimidazole and Acid with Propylene Oxide. *Green Chem.* **2003**, *5*, 731−736.
(45) Yang, X.; Yan, N.; Fei, Zh.; Crespo-Quesada, R. M.; Laurenczy, G.; Kiwi-Minsker, L.; Kou, Y.; Li, Y.; Dyson, P. J. Biphasic Hydrogenation over PVP Stabilized Rh Nanoparticles in Hydroxyl Functionalized Ionic Liquids. *Inorg. Chem.* **2008**, *47*, 7444−7446.
(46) Yan, N.; Yang, X.; Fei, Zh.; Li, Y.; Kou, Y.; Dyson, P. J. Solvent-Enhanced Coupling of Sterically Hindered Reagents and Aryl Chlorides Using Functionalized Ionic Liquids. *Organometallics* **2009**, *28*, 937−939.
(47) Chiou, J. Y. Z.; Chen, J. N.; Lei, J. S.; Lin, I. J. Ionic Liquid Crystals of Imidazolium Salts with a Pendant Hydroxyl Group. *J. Mater. Chem.* **2006**, *16*, 2972−2977.
(48) Pucheault, M.; Vaultier, M. Task Specific Ionic Liquids and Task Specific Onium Salts. *Top. Curr. Chem.* **2009**, *290*, 83−126.
(49) Tang, S.; Baker, G. A.; Zhao, H. Ether- and Alcohol-Functionalized Task-Specific Ionic Liquids: Attractive Properties and Applications. *Chem. Soc. Rev.* **2012**, *41*, 4030−4066.
(50) Zhang, S.; Qi, X.; Ma, X.; Lu, L.; Zhang, Q.; Deng, Y. Investigation of Cation-Anion Interaction in 1-(2-Hydroxyethyl)-3-Methylimidazolium-Based Ion Pairs by Density Functional Theory Calculations and Experiments. *J. Phys. Org. Chem.* **2012**, *25*, 248−257.
(51) Duisenberg, A. J. M.; Kroon-Batenburg, L. M. J.; Schreurs, A. M. M. An Intensity Evaluation Method: EVAL-14. *J. Appl. Crystallogr.* **2003**, *36*, 220−229.
(52) Blessing, R. H. An Empirical Correction for Absorption Anisotropy. *Acta Crystallogr., Sect. A* **1995**, *51*, 33−38.

(53) Sheldrick, G. M. A Short History of SHELX. *Acta Crystallogr., Sect. A* **2008**, *64*, 112−122.
(54) Frisch, M. J.; et al. *Gaussian 03*, revision B.05; Gaussian, Inc.: Wallingford, CT, 2004.
(55) Becke, A. D. Density-Functional Thermochemistry. III. The Role of Exact Exchange. *J. Chem. Phys.* **1993**, *98*, 5648−5652.
(56) Lee, C.; Yang, W.; Parr, R. G. Development of the Colle-Salvetti Correlation-Energy Formula into a Functional of the Electron Density. *Phys. Rev.* **1988**, *B37*, 785−789.
(57) Feng, S.; Li, T. Predicting Lattice Energy of Organic Crystals by Density Functional Theory with Empirically Corrected Dispersion Energy. *J. Chem. Theory Comput.* **2006**, *2*, 149−156.
(58) Civalleri, B.; Zicovich-Wilson, C. M.; Valenzano, L.; Ugliengo, P. B3LYP Augmented With an Empirical Dispersion Term (B3LYP-D*) as Applied to Molecular Crystals. *Cryst. Eng. Comm.* **2008**, *10*, 405−410.
(59) King, M. D.; Buchanan, W. D.; Korter, T. M. Application of London-Type Dispersion Corrections to the Solid-State Density Functional Theory Simulation of the Terahertz Spectra of Crystalline Pharmaceuticals. *Phys. Chem. Chem. Phys.* **2011**, *13*, 4250−4259.
(60) Fedorov, I. A.; Zhuravleva, Y. N.; Berveno, V. P. Electronic Structure and Chemical Bond in Naphthalene and Anthracene. *Phys. Chem. Chem. Phys.* **2011**, *13*, 5679−5686.
(61) Grimme, S.; Antony, J.; Ehrlich, S.; Krieg, H. A Consistent and Accurate Ab Initio Parametrization of Density Functional Dispersion Correction (DFT-D) for the 94 Elements H-Pu. *J. Chem. Phys.* **2010**, *132*, 154104.
(62) Grimme, S.; Ehrlich, S.; Goerigk, L. Effect of the Damping Function in Dispersion Corrected Density Functional Theory. *J. Comput. Chem.* **2011**, *32*, 1456−1465.
(63) http://www.thch.uni-bonn.de/tc/.
(64) Grimme, S.; Hujo, W.; Kirchner, B. Performance of Dispersion-Corrected Density Functional Theory for the Interactions in Ionic Liquids. *Phys. Chem. Chem. Phys.* **2012**, *14*, 4875−4883.
(65) Akin-Ojo, A.; Wang, F. Effects of the Dispersion Interaction in Liquid Water. *Chem. Phys. Lett.* **2011**, *513*, 59−62.
(66) Zvereva, E.; Shagidullin, A. R.; Katsyuba, S. A. Ab Initio and DFT Predictions of Infrared Intensities and Raman Activities. *J. Phys. Chem. A* **2011**, *115*, 63−69.
(67) Dovesi, R.; Saunders, V. R.; Roetti, C.; Orlando, R.; Zicovich-Wilson, C. M.; Pascale, F.; Civalleri, B.; Doll, K.; Harrison, N. M.; Bush, I. J. D'Arco, Ph.; Llunell, M. et al. *Crystal06 User's Manual*; Universita di Torino: Torino, 2006.
(68) Pascale, F.; Zicovich-Wilson, C. M.; Gejo, F. L.; Civalleri, B.; Orlando, R.; Dovesi, R. The Calculation of the Vibrational Frequencies of Crystalline Compounds and Its Implementation in the CRYSTAL Code. *J. Comput. Chem.* **2004**, *25*, 888−897.
(69) Zicovich-Wilson, C. M.; Dovesi, R.; Saunders, V. R. A General Method to Obtain Well Localized Wannier Functions for Composite Energy Bands in Linear Combination Of Atomic Orbital Periodic Calculations. *J. Chem. Phys.* **2001**, *115*, 9708−9719.
(70) Saunders, V. R.; Dovesi, R.; Roetti, C.; Causa, M.; Harrison, N. M.; Orlando, R.; Zikovich-Wilson, C. M. *CRYSTAL 98 User's Manual*; Universita di Torino: Torino, 1998.
(71) Gatti, C. *TOPOND98 User's Manual*; CNR-CSRSRC: Milano, Italy, 1999.
(72) Churakov, A. V.; Prikhodchenko, P. V.; Lev, O.; Medvedev, A. G.; Tripol'skaya, T. A.; Vener, M. V. A Model Proton-Transfer System in the Condensed Phase: NH_4+ OOH-, a Crystal with Short Intermolecular H-Bonds. *J. Chem. Phys.* **2010**, *133*, 164506.
(73) Vener, M. V.; Medvedev, A. G.; Churakov, A. V.; Prikhodchenko, P. V.; Tripol'skaya, T. A.; Lev, O. H-Bond Network in Amino Acid Cocrystals with H_2O or H_2O 2. The DFT Study of Serine - H_2O and Serine - H_2O 2. *J. Phys. Chem. A* **2011**, *115*, 13657−13663.
(74) See Refs. cited in Zvereva, E. E.; Katsyuba, S. A.; Dyson, P. J. A Simple Physical Model for the Simultaneous Rationalisation of Melting Points and Heat Capacities of Ionic Liquids. *Phys. Chem. Chem. Phys.* **2010**, *12*, 13780−13787.
(75) Vener, M. V.; Sauer, J. Environmental Effects on Vibrational Proton Dynamics in H_5O^{2+}: DFT Study on Crystalline $H_5O^{2+}ClO_4^-$. *Phys. Chem. Chem. Phys.* **2005**, *7*, 258−263.
(76) Zicovich-Wilson, C. M.; San-Román, M. L.; Camblor, M. A.; Pascale, F.; Durand-Niconoff, J. S. Structure, Vibrational Analysis, and Insights into Host-Guest Interactions in as-Synthesized Pure Silica ITQ-12 Zeolite by Periodic B3LYP Calculations. *J. Am. Chem. Soc.* **2007**, *129*, 11512−11523.
(77) Jezierska, A.; Panek, J. J.; Koll, A.; Mavri, J. Car-Parrinello Simulation of an O-H Stretching Envelope and Potential of Mean Force of an Intramolecular Hydrogen Bonded System: Application to a Mannich Base in Solid State and in Vacuum. *J. Chem. Phys.* **2007**, *126*, 205101.
(78) Vener, M. V.; Manaev, A. V.; Tsirelson, V. G. Proton Dynamics in Strong (Short) Intramolecular H-Bond. DFT Study of the KH Maleate Crystal. *J. Phys. Chem. A* **2008**, *112*, 13628−13632.
(79) Jezierska-Mazzarello, A.; Vuilleumier, R.; Panek, J. J.; Ciccotti, G. Molecular Property Investigations of an Ortho-Hydroxy Schiff Base Type Compound with the First-Principle Molecular Dynamics Approach. *J. Phys. Chem. B* **2010**, *114*, 242−253.
(80) King, M. D.; Korter, T. M. Effect of Waters of Crystallization on Terahertz Spectra: Anhydrous Oxalic Acid and Its Dehydrate. *J. Phys. Chem. A* **2010**, *114*, 7127−7138.
(81) Vener, M. V.; Egorova, A. N.; Tsirelson, V. G. Hydrogen Bonds and O···O Interactions in Proton-Ordered Ices. DFT Computations with Periodic Boundary Conditions. *Chem. Phys. Lett.* **2010**, *500*, 272−276.
(82) Tsuzuki, S.; Orita, H.; Honda, K.; Mikami, M. First-Principles Lattice Energy Calculation of Urea and Hexamine Crystals by a Combination of Periodic DFT and MP2 Two-Body Interaction Energy Calculations. *J. Phys. Chem. B* **2010**, *114*, 6799−6805.
(83) Brela, M.; Stare, J.; Pirc, G.; Sollner-Dolenc, M.; Boczar, M.; Wojcik; Mavri, J. Car-Parrinello Simulation of the Vibrational Spectrum of a Medium Strong Hydrogen Bond by Two-Dimensional Quantization of the Nuclear Motion: Application to 2-Hydroxy-5-Nitrobenzamide. *J. Phys. Chem. B* **2012**, *116*, 4510−4518.
(84) Espinosa, T.; Alkorta, I.; Elguero, J.; Molins, E. From Weak to Strong Interactions: a Comprehensive Analysis of the Topological and Energetic Properties of the Electron Density Distribution Involving X-H···F-Y Systems. *J. Chem. Phys.* **2002**, *117*, 5529−5542.
(85) Gatti, C. Chemical Bonding in Crystals: New Directions. *Z. Kristallogr.* **2005**, *220*, 399−457.
(86) Vener, M. V.; Manaev, A. V.; Egorova, A. N.; Tsirelson, V. G. QTAIM Study of Strong H-Bonds with the O−H···A Fragment (A = O, N) in Three-Dimensional Periodical Crystals. *J. Phys. Chem. A* **2007**, *111*, 1155−1162.
(87) Jeffrey, G. A.; Saenger, W. *Hydrogen bonding in biological structure*; Springer-Verlag: Berlin, 1991.
(88) Steiner, T. The Hydrogen Bond in the Solid State. *Angew. Chem., Int. Ed.* **2002**, *41*, 48−76.
(89) Cammarata, L.; Kazarian, S. G.; Salter, P. A.; Welton, T. Molecular States of Water in Room Temperature Ionic Liquids. *Phys. Chem. Chem. Phys.* **2001**, *3*, 5192−5200.
(90) Kristiansson, O.; Schuisky, M. Interaction between Methanol and the Cl^-, Br^-, I^-, NO_3^-, ClO_4^-, BF_4^-, $SO_3CF_3^-$ and PF_6^- Anions Studied by FTIR Spectroscopy. *Acta Chem. Scand.* **1997**, *51*, 270−273.
(91) Small amount of water was absorbed by $[C_2OHmim][PF_6]$, when the IL was deliberately exposed to wet air for approximately one hour.
(92) Doroshenko, I.; Pogorelov, V.; Sablinskas, V.; Balevicius, V. Matrix-Isolation Study of Cluster Formation in Methanol: O-H Stretching Region. *J. Mol. Liq.* **2010**, *157*, 142−145.
(93) Max, J.-J.; Chapados, C. Infrared Spectroscopy of Methanol-Hexane Liquid Mixtures. II. The Strength of Hydrogen Bonding. *J. Chem. Phys.* **2009**, *130*, 124513.
(94) The scaling factor value of 0.964 was obtained from comparison of B3LYP/6-31G** computed νOH frequency of methanol (3824 cm^{-1}) with the corresponding experimental frequency of methanol in

gas phase (3687 cm^{-1}). The obtained value was used for scaling of the computed frequencies of OH and CH stretching vibrations of [C_2OHmim] cation.
(95) Lehmann, S. B. C.; Roatsch, M.; Schöppke, M.; Kirchner, B. On the Physical Origin of the Cation-Anion Intermediate Bond In Ionic Liquids Part I. Placing A (Weak) Hydrogen Bond between Two Charges. *Phys. Chem. Chem. Phys.* **2010**, *12*, 7473−7486.
(96) These effects probably explain "unusual" blue shift of νC2D band in IR spectra of solid [Emim-d]Br and [Emim-d]Tf_2N relative to the spectra of the melts, described in ref 20.
(97) Ermolaev, V.; Miluykov, V.; Krivolapov, D.; Rizvanov, I.; Zvereva, E.; Katsyuba, S.; Sinyashin, O.; Schmutzler, R. Phosphonium Ionic Liquids Based on Bulky Phosphines: Synthesis, Structure and Properties. *Dalton Trans.* **2010**, *39*, 5564−5571.
(98) Wulf, A.; Fumino, K.; Ludwig, R. Spectroscopic Evidence for an Enhanced Anion-Cation Interaction from Hydrogen Bonding in Pure Imidazolium Ionic Liquids. *Angew. Chem., Int. Ed.* **2010**, *49*, 449−453.
(99) The only structure 1 was optimized at B3LYP/6-31+G** level in ref 50. Five variants of ion pairing were found therein for [C_2OHmim][acetate]; they resemble structures 2, 3, 5, 7, and 8 from Figure 5 of present paper.
(100) Kossman, S.; Thar, J.; Kirchner, B.; Hunt, P. A.; Welton, T. Cooperativity in Ionic Liquids. *J. Chem. Phys.* **2006**, *124*, 174506.
(101) Golubev, N. S.; Denisov, G. S.; Macholl, S.; Smirnov, S. N.; Shenderovich, I. G.; Tolstoy, P. M. NMR study of blue-shifting hydrogen bonds formed by fluoroform in solution. *Z. Phys. Chem.* **2008**, *222*, 1225−1245.
(102) Lorente, P.; Shenderovich, I. G.; Golubev, N. S.; Denisov, G. S.; Buntkowsky, G.; Limbach, H.-H. 1H/15N NMR chemical shielding, dipolar 15N,2H coupling and hydrogen bond geometry correlations in a novel series of hydrogen-bonded acid-base complexes of collidine with carboxylic acids. *Magn. Reson. Chem.* **2001**, *39*, S18−S29.
(103) Seduraman, A.; Wu, P.; Klahn, M. Extraction of Tryptophan with Ionic Liquids Studied with Molecular Dynamics Simulations. *J. Phys. Chem. B* **2012**, *116*, 296−304.
(104) Klahn, M.; Lim, G. S.; Wu, P. How Ion Properties Determine the Stability of a Lipase enzyme in ionic liquids: A Molecular Dynamics Study. *Phys. Chem. Chem. Phys.* **2011**, *13*, 18647−18660.
(105) Klahn, M.; Seduraman, A.; Wu, P. Proton Transfer between Tryptophan and Ionic Liquid Solvents Studied with Molecular Dynamics Simulations. *J. Phys. Chem. B* **2011**, *115*, 8231−8241.
(106) Stare, J.; Mavri, J.; Grdadolnik, J.; Zidar, J.; Maksić, Z. B.; Vianello, R. Hydrogen Bond Dynamics of Histamine Monocation in Aqueous Solution: Car-Parinello Molecular Dynamics and Vibrational Spectroscopic Study. *J. Phys. Chem. B* **2011**, *115*, 5999−6010.